Dynamical properties of heavy-ion reactions deduced from coupled-channels calculations

D. Pelte* and U. Smilansky
The Weizmann Institute of Science, Rehovot, Israel
(Received 3 October 1978)

The distribution of the total reaction, fusion, and direct reaction cross section in $\vec{I}$ space are studied using coupled-channels calculations. These calculations also provide information about such quantities as the polarization of highly excited states, the energy dependence of the fusion cross section, and the dependence of the total kinetic energy loss on the spins of the excited states.

[NUCLEAR REACTIONS Model coupled-channels calculations; deduced σ_R, σ_F, σ_D, polarization; dependence on angular momentum transfer and interactions.]

I. INTRODUCTION

The decomposition of the angular momentum space of the incoming wave into fractions each representing a particular type of reaction (fusion, deeply inelastic, quasielastic) appears to be one of the fundamental problems in the interpretation of experimental results from heavy ion reactions. For example, this decomposition is used in the interpretation of (HI, xn) reactions,[1] and it is also required in the technique of Ref. 2 where the deflection functions of deeply inelastic reactions are extracted. The usual method of decomposition should be considered as rather intuitive: The initial angular momentum distribution is fractionated into sharp bins for each type of reaction. Although it is conceded that the sharp cutoff assumption is only a rough approximation, the more important question is whether or not each reaction type is indeed correlated to an approximately exclusive range of angular momenta where the contribution to other reactions can be neglected. In the case of compound-nucleus reactions, the experimental evidence[3,4] seems to indicate that this is not true. The compound-nucleus reactions are unique in the sense that all the orbital angular momentum in the entrance channel is converted to internal spin. The latter can be experimentally deduced by, e.g., measuring the multiplicities of the de-exciting γ rays. In all other cases of heavy ion reactions the incoming angular momenta are distributed among internal spins of the products *and* their orbital angular momenta. It is therefore impossible to relate the residual spins of the products, even if they can be measured, to any particular incoming orbital angular momentum.

The relation between the initial angular momentum and the reaction channels could be studied theoretically within an appropriate model. Since realistic models are not solvable with present day techniques, we have to resort to simplified models in which some of the relevant features are properly treated. In the present paper we discuss the results of such calculations. In order to understand the effect of the angular momentum and energy transfer, we solve a coupled-channels system, in which the direct reactions are represented by collective excitations along a level sequence with excitation energies similar to those of the yrast band. Compound-nucleus channels are taken into account by the imaginary part of the optical interaction. By changing the spin sequence of the excited levels or the strength of the interaction in the optical model, we are able to study the effect of the various factors on measurable quantities. These are, e.g., the compound and total reaction cross sections, average kinetic energy loss, residual polarization and alignment of the reaction products and their dependence on the bombarding energy. Apart from this information we get a detailed picture of the role played by the various values of the incoming angular momenta in determining the above mentioned quantities. We discovered that the general conclusions from these model calculations can be understood in terms of simple physical concepts. We therefore believe that the validity of these conclusions goes beyond the narrow range of the model and may apply to more general processes which can occur in the reactions between heavy ions.

Throughout this study we neglected the possibility that the imaginary part of the optical model potential may depend on the incoming angular momentum. Such dependence is usually introduced in order to take into account the sharp drop of the nuclear state density at the yrast line. This effect was not considered in the present study because the knowledge of how to incorporate the nuclear state density into the properties of the imaginary potential is rather rudimentary and because we mainly wanted to isolate the dynamical effects due to the *direct* coupling of excited states and spins.

II. COMPUTATIONAL PROCEDURES

The technique of coupled channels is well known and needs not be described here. For an introduction the reader is referred to Refs. 5, 6. The coupled-channels program that was used in the present investigation is based on the formulation of Ref. 7 and uses the same phase conventions. The program makes use of some computational modifications that were described by Raynal.[8] The code is written in such a way that it can handle up to 36 angular momenta in the exit channels that couple to a given value of the initial angular momentum. This number of couplings allows one to treat, for example, a $K^\pi = 0^+$ rotational band up to the $I^\pi = 10^+$ member. The output of the code consists of the S matrix $S^J_{I_i l_i; I_f l_f}$, where J is the total angular momentum and I_i, I_f are the spins of the target in the initial or final states and l_i, l_f are the relative angular momenta in the entrance or exit channels. We assume that only the target (or projectile) is excited by the reaction and that the ground states of target and projectile have $I^\pi = 0^+$.

The S matrix $S^{I_i}_{0 l_i; I_f l_f}$ is the basic quantity from which one may calculate other quantities such as the scattering amplitudes $f_{I_f M_f}(\theta_{sc})$ [see Eq. (4) of Ref. 7] or the integrated cross section σ_{I_f} for the excitation of a specific final state with spin I_f. This cross section is given by

$$\sigma_{I_f} = \frac{4\pi}{K_f^2} \sum_{l_i l_f} (2l_f + 1) \left| S^{I_i}_{0 l_i; I_f l_f} \right|^2 ,$$

where K_f is the wave number of the exit channel. This may also be written as

$$\sigma_{I_f} = \sum_{l_i} \sigma_{I_f l_i} = \sum_{l_f} \sigma_{I_f l_f} ,$$

where

$$\sigma_{I_f l_i} = \frac{4\pi}{K_f^2} \sum_{l_f} (2l_f + 1) \left| S^{I_i}_{0 l_i; I_f l_f} \right|^2$$

and

$$\sigma_{I_f l_f} = \frac{4\pi}{K_f^2} (2l_f + 1) \sum_{l_i} \left| S^{I_i}_{0 l_i; I_f l_f} \right|^2 .$$

The total inelastic cross section which, in our model, represents the population of channels by the direct process is given by

$$\sigma_D = \sum_{I_f}{}' \sigma_{I_f} ,$$

where the prime indicates that the ground state is not included in the summation.

The average initial angular momentum that contributes to the excitation of the final state is

$$\langle l_i \rangle_{I_f} = \frac{\sum_{l_i} l_i \sigma_{I_f l_i}}{\sigma_{I_f}}$$

and for the average final angular momentum one has

$$\langle l_f \rangle_{I_f} = \frac{\sum_{l_f} l_f \sigma_{I_f l_f}}{\sigma_{I_f}} .$$

The other important quantity is the total reaction cross section. It is expressed in the terms of the S matrix elements as

$$\sigma_R = \frac{4\pi}{K_i^2} \sum_{l_i} (2l_i + 1)(\mathrm{Im} S^{l_i}_{0 l_i; 0 l_i} - \left| S^{l_i}_{0 l_i; 0 l_i} \right|^2) .$$

The σ_R is composed of two contributions. The first is σ_D introduced above. The second is the contribution from direct processes which are not treated explicitly and other processes like the compound-nucleus formation. Assuming that σ_D exhausts all the direct contributions and that the most important fraction of the remaining flux goes into fusion reactions, one obtains

$$\sigma_F = \sigma_R - \sigma_D .$$

Finally, one may also study the degree of alignment and polarization of a final state that was excited by the reaction. These may be deduced from the density matrix

$$\rho^{(I_f)}_{M_f M_f'}(\theta_{sc}) = f_{I_f M_f}(\theta_{sc}) f^*_{I_f M_f'}(\theta_{sc}) .$$

The classical models of heavy ion reactions predict[9] that the spins of the residual fragments will be polarized in the direction perpendicular to the reaction plane. The complete polarization in this classical picture requires that the density matrix be real and diagonal in the coordinate system C_p which has its z axis parallel to $\vec{K}_i \times \vec{K}_f$. We thus should have

$$\tilde{\rho}^{(I_f)}_{M_f M_f'}(\theta_{sc}) = \sum_{m_f m_f'} \mathfrak{D}^{I_f}_{M_f m_f} \rho^{(I_f)}_{m_f m_f'}(\theta_{sc}) \mathfrak{D}^{I_f *}_{M_f' m_f'} = P_{M_f} \delta_{M_f M_f'} . \quad (1)$$

The rotation matrix $\mathfrak{D}^{I_f}_{M_f m_f}$ rotates the original system where z is parallel to the beam axis, into the system C_p. On the other hand, if the states are completely aligned, the same result applies with the additional condition $P_{M_f} = P_{-M_f}$.

The calculations were performed for the reaction $^{12}C + {}^{24}Mg$ at several bombarding energies between 13.3 and 90.9 MeV (all energies are given in the c.m. system). Two sets of states were considered. The first set, Y, consists of a rotational band with members at the following excitation energies: 0^+,

0 MeV; 2^+, 1.37 MeV; 4^+, 4.12 MeV; 6^+, 8.12 MeV; 8^+, 13.9 MeV; 10^+, 21 MeV. The second set, 0, has states with spin 0^+ at the same excitation energies. The number of 0^+ states at a particular energy is equal to I_f+1, where I_f is the spin of the corresponding rotational state at the same excitation energy. Furthermore, the matrix elements that couple the different states in each set have the same magnitude and radial dependence. In this way one can study the influence of level spins on the properties of the reaction keeping all other quantities (coupling strength, excitation energies etc.) unchanged.

The form factors of the real and imaginary part of the nuclear potential were assumed to have Fermi shapes:

$$V(R)=\frac{U}{1+\exp[(R-R_u)/a_u]}+\frac{iW}{1+\exp[(R-R_w)/a_w]}+V_c,$$

where V_c represents the Coulomb potential. The coupling form factor was determined by the first derivative of the real part of the nuclear potential. The total strengths of the coupling matrix elements were calculated within the rotational model[5] by using a quadrupole deformation of $\beta_2=0.4$. These matrix elements were kept constant in all the calculations. It should also be noted that the Coulomb excitation was not included in the calculations. Thus the upper limit in the integration of the Schrödinger equation was R_u+20a_u. It was checked on several occasions that an increase of this limit left the S matrix elements unchanged.

The parameters of the optical model were $R_u=6.98$ fm, $a_u=0.60$ fm, $a_w=0.60$ fm, and $W=-5$ MeV. The values of U and R_w were varied. Two alternative values of U and two alternative values of R_w were used. Altogether we considered four optical model sets. We denote them by the letters N, C, S, and I. The letters N and C stand for the value of U, which is $U=-50$ MeV for set N and $U=0$ MeV for set C. Similarly $R_w=6.98$ fm for set S and $R_w=5.17$ fm for set I. Thus the potential NI has $U=-50$ MeV and $R_w=5.17$ fm, and so on. The set C was chosen in order to study qualitatively, in what way the dominance of the Coulomb interaction determines the properties of heavy ion reactions. The change of R_w was mainly introduced to see whether or not the concept of a critical radius introduced by Galin *et al.*[10] is also valid in these coupled-channels calculations. We were also interested to see by how much the coupling of the directly accessible states changes the behavior of the fusion cross section. These last two problems are closely related to the model of Glas *et al.*[11] which is frequently used to interpret measured fusion cross sections.

For a given bombarding energy, eight calculations with different sets of optical parameters and coupled states were carried out. These calculations are labeled by, e.g., *YNS*, the symbols specifying the particular level sequence and parameter set that was used. Before proceeding to the next section it should be mentioned that we also investigated various approximate methods to solve the coupled-channels problem. Similar problems to the ones encountered here (a large number of states that can be excited) are also familiar in molecular physics and several approximations were developed in this field. The most commonly used approximations are the P-helicity decoupling approximation[12] and the dominant-l approximation.[13] Both methods consist of reducing the $\vec{l}$ space that may become prohibitively large when high-spin states are coupled. In our case the coupled-channels calculations become unfeasible when a 12^+ state is coupled to the 10^+ states. The reduction of $\vec{l}$ space, with a simultaneous increase in level space, is thus an alternative to the more commonly used technique where the level space is truncated but all angular momenta are considered. It was checked systematically either by using the p-helicity decoupling or dominant-l approximations or by reducing the number of coupled states that the truncation of the level space, with all l values included, affects the calculated values of σ_R and σ_D least. It is estimated from this study that the deviations of σ_R and σ_D from their exact values are smaller than 10% at the largest bombarding energies where the truncation of the level space is probably of greatest influence.

III. RESULTS AND DISCUSSION

The results of the calculations are arranged into five subsections, each of which emphasizes a particular aspect of the reaction dynamics.

A. Energy dependence of the total reaction and fusion cross sections

The total reaction cross sections increase with increasing bombarding energy, and this energy dependence is almost independent of the optical parameter set (cf. Fig. 1). At the largest bombarding energy of 90.9 MeV the total reaction cross sections are roughly 2 b and they approach zero at an incident energy of approximately 10 MeV. On the other hand, the fusion cross sections depend strongly on the shape of the optical potential and, to a less extent, also on the spins of the states that are directly coupled to the entrance channel. From Fig. 1 one recognizes two conditions for obtaining a small fusion cross section: Either the Coulomb interaction dominates the potential or the absorption radius is small. The

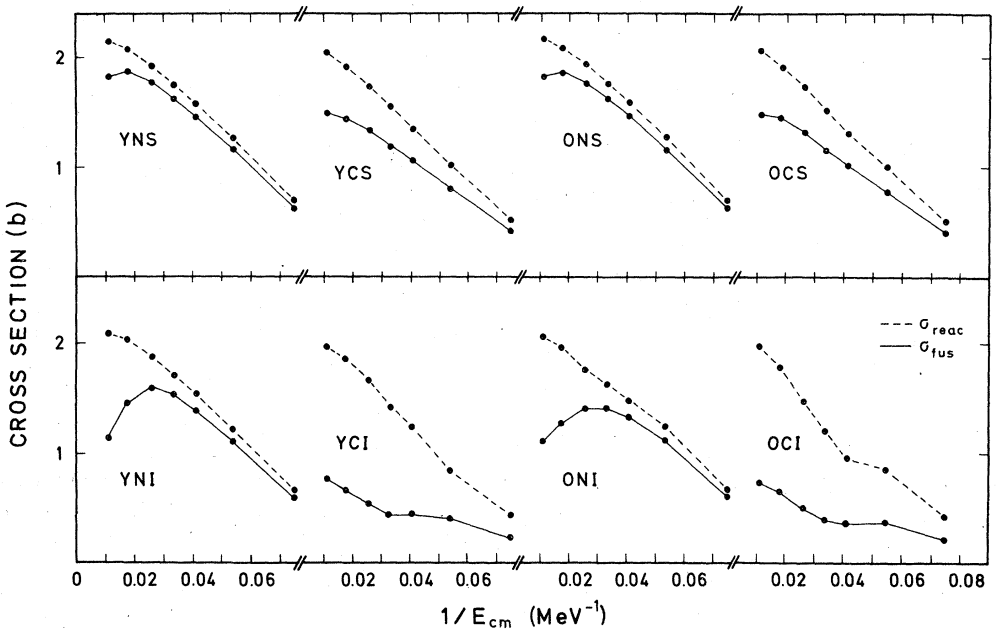

FIG. 1. Calculated total reaction and fusion cross sections. For the potential parameter sets see text.

latter condition is particularly important at high incident energies and is responsible for the decrease of the calculated σ_F with increasing energy for some of the parameter sets. This behavior of σ_F is experimentally observed in reactions between light heavy ions (cf. Ref. 11) and usually interpreted in terms of the model of Glas *et al.*[11]

The model of Glas *et al.* predicts a simple energy dependence of the fusion cross section at high and low bombarding energies

$$\sigma_F = \begin{cases} \pi R_{\text{in}}^2(1 - V_{\text{in}}/E), & E \gg E_c \\ \pi R_{\text{out}}^2(1 - V_{\text{out}}/E), & E \ll E_c \end{cases} \tag{2}$$

where the quantity E_c is defined by Eq. (19) of Ref. 11. At high energies the cross section is determined by a critical radius R_{in} and the value of the real part of the combined nuclear and Coulomb potentials at this radius. We thus see that the sign of the slope $d\sigma_F/d(1/E)$ depends on whether the value of V_{in} is positive or negative. At the other extreme energy range, the parameter which determines the behavior of the fusion cross section is R_{out}, where the combined real part of the nuclear and Coulomb potentials attains its maximum value V_{out}.

The results of the present calculations are consistent with the simple parametrization of Glas *et al.*[11] In Table I we display the values of R_{in}, V_{in}, R_{out}, and V_{out} obtained by extrapolating the results of the calculations to the limits $1/E = 0$ or $\sigma_F = 0$, respectively. These values are compared with R_w, $\text{Re}[V(R_w)]$, $R_{\text{out}}^{\text{opt}}$ and $\text{Re}[V(R_{\text{out}}^{\text{opt}})]$ which are derived from the optical potential. Deviations of 15% in the R parameters and of 40 MeV in the V parameters are observed. Nevertheless, and considering the simplicity of the model of Glas *et al.*, one is led to the conclusion that this model works

TABLE I. Comparison of critical radii and potentials, deduced from the fusion cross sections, with the input parameters of the calculations. For the abbreviations see text.

Parameter set	R_{in} (fm)	V_{in} (MeV)	R_w (fm)	$\text{Re}[V(R_w)]$ (MeV)	R_{out} (fm)	V_{out} (MeV)	$R_{\text{out}}^{\text{opt}}$ (fm)	$\text{Re}[V(R_{\text{out}}^{\text{opt}})]$ (MeV)
YNS	7.45	−3.9	6.98	−10.2	8.90	15.0	10.35	10.5
YCS	7.04	4.7	6.98	14.8	7.71	15.5		
YNI	4.50	−70.9	5.17	−29.4	8.90	15.0	10.35	10.5
YCI	5.54	17.9	5.17	18.2	5.23	14.8		
ONS	7.50	−2.2	6.98	−10.2	8.90	15.0	10.35	10.5
OCS	6.93	2.6	6.98	14.8	7.71	15.5		
ONI	5.02	−34.0	5.17	−29.4	8.90	15.0	10.35	10.5
OCI	5.33	14.5	5.17	18.2	5.23	14.8		

surprisingly well. In particular the slope of the fusion cross section at large bombarding energies appears to indicate whether or not the combined nuclear and Coulomb potentials are attractive or repulsive inside the nucleus. It seems particularly important that this information is free of the ambiguities that one encounters in the analysis of elastic and inelastic scattering. On the other hand, it should be realized that the fusion cross section also follows the parametrization (2) if one of the conditions used in the model of Glas *et al.*,[11] namely the existence of a potential barrier at $R_{\text{out}}^{\text{opt}}$, is not fulfilled (cf. the results for the parameter set C in Table I).

When the Coulomb interaction dominates, the calculated fusion cross section decreases. This result is in accordance with the experimental observation (cf. Ref. 14) that σ_F is negligibly small for heavy systems. In addition other mechanisms like the existence of the yrast limit also reduce σ_F. It was pointed out above that this latter mechanism was not included in the present calculation.

B. l_i distribution of the fusion cross section

Usually it is assumed that the fusion cross section exhausts the total reaction cross section for incident l_i values below a critical value l_{cr} and that the total reaction cross section is equivalent to the direct reaction cross section for $l_{\text{cr}} < l_i < l_{\text{max}}$. With these assumptions one obtains l_{max} and l_{cr} through the relations

$$\sigma_R = \frac{\pi}{K_i^2}(l_{\text{max}}+1)^2, \tag{3a}$$

$$\sigma_F = \frac{\pi}{K_i^2}(l_{\text{cr}}+1)^2. \tag{3b}$$

For four selected parameter sets the distributions $d\sigma_R/dl_i$ and $d\sigma_F/dl_i$ are shown in Fig. 2. Note that these results were averaged over an interval of five l_i units in order to remove the effects of shape resonances in the potential well. These resonances seem to develop if the damping in the surface region of the potential is too weak. Apparently, the direct coupling of 36 partial waves does not provide sufficient damping. The occurrence of resonances is interesting and may be related to the correlated structures that were observed experimentally in the fusion cross sections of the reactions $^{12}C+^{12}C$ (Ref. 15), $^{12}C+^{16}O$ (Ref. 16), and $^{16}O+^{16}O$ (Ref. 17). This aspect of the calculations was not investigated further.

It is evident from Fig. 2 that the slopes of $d\sigma_R/dl_i$ at large angular momenta are quite similar regardless of the potential parameter set or level sequence. Thus Eq. (3a) appears to provide a useful estimate of the maximum angular momentum that contributes to σ_R. On the other hand, the corresponding slopes of $d\sigma_F/dl_i$ are very different and depend on the fusion probability. It is found that the calculated $d\sigma_F/dl_i$ is of nearly triangular shape with lower and upper l_i limits of $l_i = 0$ and $l_i = l_{\text{max}}$, respectively. The angular momentum l_{fus} for which $d\sigma_F/dl_i$ reaches a maximum is given approximately by

$$l_{\text{fus}} = \frac{l_{\text{max}}[\alpha(l_{\text{max}}+2)-\frac{1}{2}]+\alpha-1}{l_{\text{max}}+\frac{3}{2}}, \tag{4}$$

where $\alpha = \sigma_F/\sigma_R$ is the ratio between the fusion and total reaction cross sections. [Note that $l_{\text{fus}} = l_{\text{max}}$ for $\alpha = 1$, but that $\alpha = 0$ is not consistent with the derivation of Eq. (4).] For $l_i \leq l_{\text{fus}}$ the fusion cross section is almost equal to the total reaction cross

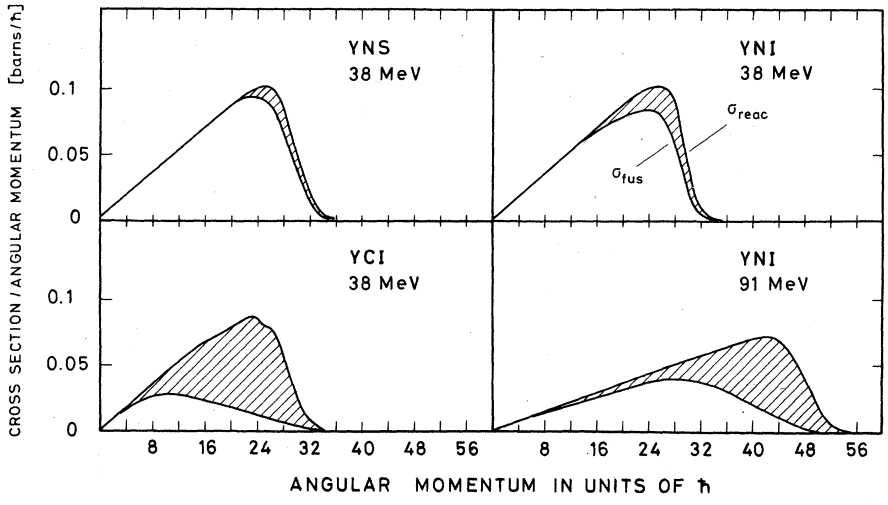

FIG. 2. Calculated distributions of the total reaction and fusion cross sections in the $\vec{l}_i$ space. The shaded areas correspond to the direct reaction cross sections. For the potential parameter sets see text.

section. One thus has to conclude that the sharp cutoff approximation made to obtain Eq. (3a) cannot be used with similar confidence for the fusion cross section Eq. (3b). The inadequacy of this approximation depends on α, the ratio between fusion and total reaction cross sections.

The broad distribution of σ_F in angular momentum space was experimentally observed by Hageman *et al.*[3] and Sarantites *et al.*[4] who investigated the reaction $^{16}O+^{148,150}Nd$ and $^{20}Ne+^{150}Nd$, respectively. As mentioned above, the assumption of a sharp cutoff in the $d\sigma_F/dl_i$ distribution should become worse the smaller the fusion cross section is with respect to the total reaction cross section. In the experiments mentioned above the fusion cross sections amounted to more than 70% of the reaction cross sections, which cannot be considered as a small fraction. Experiments with other systems having a relatively smaller σ_F are crucial in order to support the conclusions from the present calculation. Note, however, that the yrast limit might modify the l_i distribution of the fusion cross section.

C. l_i and l_f distributions of the direct reaction cross sections

The quantities $\sigma_{I_f l_i}$ and $\sigma_{I_f l_f}$ display broad distributions in the spaces of l_i and l_f, respectively. This is shown in Fig. 3 for two selected parameter sets. The corresponding mean values $\langle l_i \rangle_{I_f}$ and $\langle l_f \rangle_{I_f}$ are presented in Table II. These values are expected to be influenced by the resonance phenomena mentioned above. Nevertheless, at close inspection of Table II one may deduce some general trends in the behavior of $\langle l_i \rangle_{I_f}$ and $\langle l_f \rangle_{I_f}$. The mean values $\langle l_i \rangle_{I_f}$ depend, for a given excitation energy and optical potential, on the spins I_f. It is found that $\langle l_i \rangle_{I_f}$ only slightly changes with excitation energy if the excited states belong to the rotational band. But $\langle l_i \rangle_{I_f}$ decreases strongly with increasing excitation energies if all excited states have spin 0^+. On the other hand, Table II suggests that $\langle l_f \rangle_{I_f}$ is nearly independent of the spin of the excited states but depends on their excitation energies. It also appears that a small fusion cross section tends to reduce the values of $\langle l_i \rangle_{I_f}$ and $\langle l_f \rangle_{I_f}$

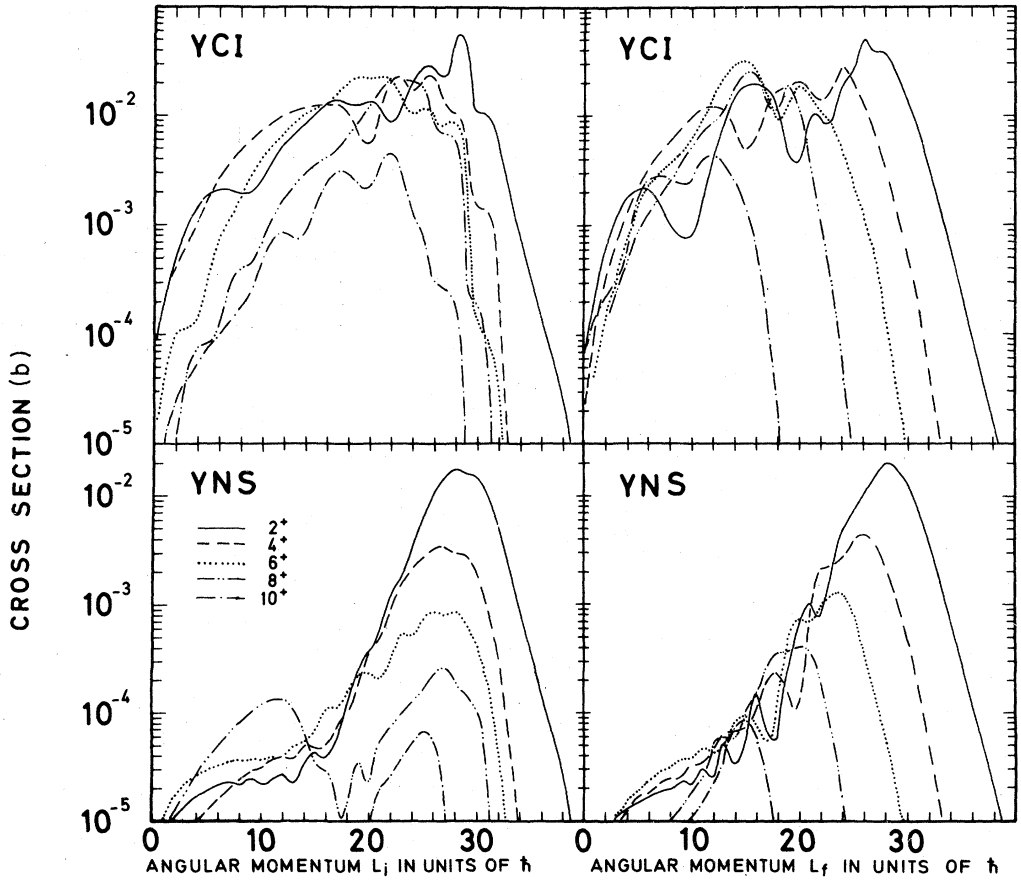

FIG. 3. Calculated distributions of the direct reaction cross sections in the $\vec{l}_i$ and $\vec{l}_f$ space at 38 MeV bombarding energy. For the potential parameter sets see text.

TABLE II. Average ingoing and outgoing angular momenta for the different parameter sets (see text) and excited states. The incident energy is 38 MeV.

	$Q \doteq Q_{2^+}$		$Q = Q_{4^+}$		$Q = Q_{6^+}$		$Q = Q_{8^+}$		$Q = Q_{10^+}$	
	$I_f = 2^+$ $I_f = 0^+$ $\langle l_i \rangle$	(set Y) (set 0) $\langle l_f \rangle$	$I_f = 4^+$ $I_f = 0^+$ $\langle l_i \rangle$	(set Y) (set 0) $\langle l_f \rangle$	$I_f = 6^+$ $I_f = 0^+$ $\langle l_i \rangle$	(set Y) (set 0) $\langle l_f \rangle$	$I_f = 8^+$ $I_f = 0^+$ $\langle l_i \rangle$	(set Y) (set 0) $\langle l_f \rangle$	$I_f = 10^+$ $I_f = 0^+$ $\langle l_i \rangle$	(set Y) (set 0) $\langle l_f \rangle$
YNS	28.1	27.9	26.1	24.9	24.2	21.7	19.5	18.5	22.4	14.4
YCS	24.9	24.8	21.5	20.8	20.3	17.6	21.2	15.9	18.0	9.9
YNI	26.8	26.6	23.8	23.1	21.9	20.3	17.8	16.5	22.2	14.1
YCI	22.9	22.7	19.4	18.4	19.3	16.1	21.6	15.2	18.7	9.9
ONS	27.8	27.8	25.7	25.7	23.3	23.3	17.9	17.9	12.1	12.1
OCS	25.0	25.0	21.6	21.6	20.0	20.0	17.7	17.7	11.4	11.4
ONI	26.4	26.4	24.3	24.3	21.6	21.6	17.6	17.6	12.4	12.4
OCI	22.6	22.6	19.5	19.5	19.5	19.5	17.3	17.3	11.5	11.5

in other wise similar conditions (compare *YNS* with *YCS* and *YNI* with *YCI*; note, however, the exception Q_{8^+}). This latter behavior is indeed expected from the l_i dependence of σ_F as discussed in Sec. III B.

The distributions of $\sigma_{I_f l_f}$ shown in Fig. 3 and the corresponding distributions for other parameter sets indicate that $\sigma_{I_f l_f}$ becomes independent of the specific parameter set or the level sequence for large l_f values. The upper boundary $l_f^{\max}$ of the $\sigma_{I_f l_f}$ distribution only depends on the excitation energy Q and may be estimated from

$$l_f^{\max} = 0.22 R_{\text{out}}^{\text{opt}} \{\mu(E - \text{Re}[V(R_{\text{out}}^{\text{opt}})] - Q)\}^{1/2}, \quad (5)$$

where μ is the reduced mass of the exit channel. At this value of l_f the cross sections $\sigma_{I_f l_f}$ have dropped to 10–1% of their maximum values except for the 10^+ states of *YNS*, which is very weakly excited at 38 MeV bombarding energy.

The relation between $\langle l_i \rangle_{I_f}$ and $\langle l_f \rangle_{I_f}$ has to conserve angular momentum, i.e.,

$$\langle \vec{l}_i \rangle_{I_f} = \langle \vec{l}_f \rangle_{I_f} + \vec{I}_f .$$

Table II suggests that for very large excitation energies (10^+ state) and/or in cases where σ_F is small, this relation may be replaced by

$$\langle l_i \rangle_{I_f} \approx \langle l_f \rangle_{I_f} + I_f . \quad (6)$$

Under the conditions specified above, $\langle l_i \rangle_{I_f}$ is only about 10% smaller than predicted by Eq. (6). A relation of this kind is usually interpreted as saying that the internal spin I_f is perpendicular to the reaction plane. This can mean either alignment or polarization of the nuclear states. The classical picture of heavy ion reactions predicts a strong polarization. We shall show below, however, that this interpretation is not substantiated by a detailed study of the M_f state distribution.

For small excitation energies and small I_f, Eq. (6) does not seem to hold. But we found no case where $\langle l_i \rangle_{I_f} < \langle l_f \rangle_{I_f}$. Thus it appears that under all conditions one has, at least in the inelastic scattering of light heavy ions,

$$\langle l_f \rangle_{I_f} < \langle l_i \rangle_{I_f} < \langle l_f \rangle_{I_f} + I_f .$$

It should be noted that the broad distributions of $\sigma_{I_f l_i}$ disagree with the usual assumption that each Q-value bin can be related to a corresponding l_i window where contributions to other Q values are of minor importance. It seems a better approximation of our case to assume that the ratios $(\sigma_{I_f' l_i})/(\sigma_{I_f l_i})$ are independent of l_i for $l_i \leqq \min(l_i^{\max})$ where $l_i^{\max} = l_f^{\max} + I_f$. The magnitude of these ratios seems to alter from case to case, and our calculations are not conclusive enough to relate the ratios to other parameters such as the multiplicity of the excitation.

D. Dependence of the direct reaction and fusion cross sections on the spins of the directly excited states

The calculations indicate that the probability to transform kinetic energy into internal excitation depends on the spins of the excited states. One may see from Fig. 4 that the average Q value of inelastic scattering is larger if the spins of the excited states are large. This behavior is apparent under all conditions but strongest if the fusion

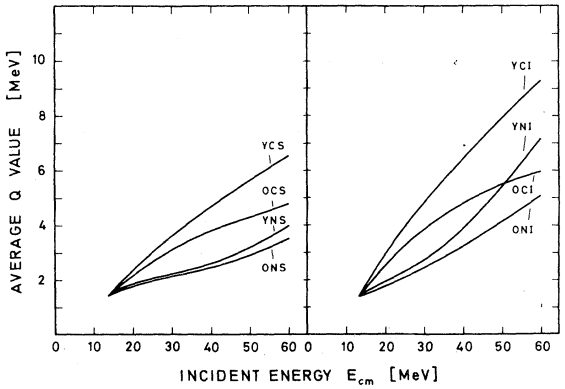

FIG. 4. Average energy loss due to the direct reactions. For the potential parameter sets see text.

cross section is small. The reason for this behavior is easy to understand: it was shown in the preceding subsection that the value of $\langle l_f \rangle_{I_f}$ is nearly independent of the actual spins of the level sequence (compare Y sets versus 0 sets). On the other hand, $\langle l_i \rangle_{I_f}$ depends strongly on the spin sequence and it is large if high spins (set Y) are considered. Thus the fraction of the total reaction cross section that can go into the excitation of a particular state can become largest if I_f attains the largest possible value. Following this argument to the extreme leads to the conclusion that a large cross section for large total kinetic energy losses is only possible if the spins of the residual fragments are large. The question of what total kinetic energy loss may be called large depends on other properties of the reaction such as the degree of deformation at the moment of separation.

There are experimental indications that high-spin states are particularly important in the dynamics of heavy ion reactions. For example, a recent study of the $^{12}C + ^{24}Mg$ reaction[18] has shown that the yrast states are predominantly excited by the inelastic scattering. Also multiplicity measurements[19] performed in order to determine the spins of residual fragments seem to indicate that high-spin states are observed in heavy ion reactions with large probabilities. Of course, it cannot be concluded that a large $l_i^{\max}$ will necessarily yield a large cross section for the production of this particular reaction channel. Other factors such as the transition strengths or the level densities at a given Q value also have to be considered. Nevertheless, it appears that the dependence of $l_i^{\max}$ on I_f is an important factor that determines the cross sections.

It should be mentioned that also the fusion possibilities slightly increase if high-spin states are directly coupled to the entrance channel. The increase is largest if the fusion cross section is small compared to the total reaction cross section but never amounts to more than 15% in our calculations. The reason for this behavior is not easy to find. It is tempting to assume, however, that the reduction of the centrifugal barrier in the case of high-spin excitations is responsible for this result. This excitation also causes a loss of kinetic energy, but under special conditions the net result is a deeper penetration of both nuclei and an enhancement of the fusion probability. The enhancement depends on the structure of the nuclei and their optical potential: The decrease of the kinetic energy has to be compensated by a much smaller centrifugal barrier.

TABLE III. Polarization P_{I_f} and alignment A_{I_f} for the 2^+ and 10^+ states at 38 MeV incident energy. The potential parameter set is *YNS*. For the definition of P_{I_f} and A_{I_f} see text.

θ_{sc}	P_{2^+}	A_{2^+}	P_{10^+}	A_{10^+}
10	−0.312	0.222	0.255	0.458
20	0.179	0.519	0.285	0.488
30	−0.060	0.516	0.407	0.361
40	−0.156	0.529	0.096	0.823
50	0.144	0.391	−0.035	0.847
60	−0.281	0.377	0.132	0.593
70	−0.831	0.068	−0.269	0.482
80	0.207	0.631	−0.413	0.368
90	0.224	0.078	0.058	0.640
100	0.231	0.160	0.325	0.529
110	0.201	0.615	0.399	0.504
120	0.432	0.542	0.637	0.215
130	0.095	0.773	0.098	0.754
140	0.922	0.032	0.608	0.176
150	0.172	0.188	−0.057	0.674
160	0.202	0.492	−0.070	0.407
170	−0.216	0.456	−0.390	0.456

E. Polarization of excited states

It was shown in Sec. IIIC that the relation $\langle l_i \rangle_{I_f} \approx \langle l_f \rangle_{I_f} + I_f$ is approximately correct for highly excited, high-spin states. This relation implies that the corresponding nuclear states show a high degree of alignment or polarization perpendicular to the reaction plane. The classical picture of heavy ion reactions predicts a strong polarization. In order to determine the degree of polarization, we calculated the density matrices $\tilde{\rho}^{(2^+)}_{M_f M_f'}(\theta_{sc})$ and $\tilde{\rho}^{(10^+)}_{M_f M_f'}(\theta_{sc})$ in the coordinate system C_p. The incident energy was 38 MeV and the optical parameter set was *YNS*. It was verified that the $\tilde{\rho}^{(I_f)}_{M_f M_f'}(\theta_{sc})$ had the symmetry properties required for the system C_p.[20] On the other hand, $\tilde{\rho}^{(2^+)}_{M_f M_f'}(\theta_{sc})$ and $\tilde{\rho}^{(10^+)}_{M_f M_f'}(\theta_{sc})$ were nondiagonal at all scattering angles where the calculations were performed (cf. Table III). Not unexpectedly, the density matrices thus did not show the extreme classical behavior on which Eq. (1) is based. We then calculated, for the 2^+ and 10^+ states, the expectation values $\langle M(\theta_{sc}) \rangle_{I_f}$ and $\langle |M(\theta_{sc})| \rangle_{I_f}$ which are defined as

$$\langle |M(\theta_{sc})| \rangle_{I_f} = \frac{\sum_{M_f} \tilde{\rho}^{(I_f)}_{M_f M_f}(\theta_{sc}) |M_f|}{I_f \sum_{M_f} \tilde{\rho}^{(I_f)}_{M_f M_f}(\theta_{sc})}$$

and

$$\langle M(\theta_{sc}) \rangle_{I_f} = \frac{\sum_{M_f} \tilde{\rho}^{(I_f)}_{M_f M_f}(\theta_{sc}) M_f}{I_f \sum_{M_f} \tilde{\rho}^{(I_f)}_{M_f M_f}(\theta_{sc})} .$$

The quantity $A_{I_f}(\theta_{sc}) = \langle |M(\theta_{sc})| \rangle_{I_f} - \langle M(\theta_{sc}) \rangle_{I_f}$ gives the expectation value of the component of the spin projection onto the z axis that is symmetric to the reaction plane, whereas $P_{I_f}(\theta_{sc}) = \langle M(\theta_{sc}) \rangle_{I_f}$ corresponds to the component that is asymmetric to

the reaction plane. It is convenient to interpret $A_{I_f}(\theta_{sc})$ as the degree of alignment and $P_{I_f}(\theta_{sc})$ as the degree of polarization. The results, for various angles, are presented in Table III. With the exception of a few angles it is found that the 2^+ and 10^+ states are more strongly aligned than polarized. These features become even more evident if $A_{I_f}(\theta_{sc})$ and $P_{I_f}(\theta_{sc})$ are averaged over the scattering cross sections. We then find

$$\langle A_{2^+}\rangle = 0.629, \quad \langle P_{2^+}\rangle = -0.035$$

and

$$\langle A_{10^+}\rangle = 0.549, \quad \langle P_{10^+}\rangle = 0.246.$$

These results indicate that in the special cases considered here, Eq. (6) rather reflects a strong alignment than polarization.

IV. SUMMARY AND CONCLUSION

We have studied the dynamical properties of heavy ion reactions on the basis of a simplified model. The model is simplified because it does not include all the nuclear degrees of freedom, but it allows one to study the exchange of energy and angular momentum within a specified subset of nuclear states. In view of this restriction it seems obvious that a direct comparison of, for example, the calculated cross sections with experimental data was not the aim of these calculations. On the other hand, we believe that some features of our calculations, such as the coupling modes between initial and final angular momenta or the dependence of the energy exchange on the angular momentum exchange, are of a more general nature, and thus these particular aspects should be important for all heavy ion reactions.

The important result of the calculation is that the concept of sharp angular momentum bins each related to a specific type of reaction does not seem to hold. In particular, this relation does not exist for the fusion process if the assumption is made that the fusion probability is determined by a critical radius. In principle it seems that the total range of angular momenta consistent with the upper boundaries in the initial and final channels participate in building up the cross section of each reaction channel. Estimates of these angular momentum boundaries are the following: (i) The maximum angular momentum l_{max} may be estimated from the reaction cross section by means of Eq. (3a). As expected, the $d\sigma_R/dl_i$ distributions show a certain degree of diffuseness in the angular momentum range around l_{max}. It was shown in the preceding paragraph that the slope of $d\sigma_R/dl_i$ in this range is very nearly independent of the potential and the directly excited states. (ii) The partial fusion cross sections $d\sigma_F/dl_i$ extend from $l_i = 0$ to $l_i = l_{max}$ and reach a maximum value at $l_i = l_{fus}$ that may be calculated with the help of Eq. (4). For $l_i \leq l_{fus}$ the fusion cross section is almost equal to the total reaction cross section. (iii) The maximum value of the exit angular momenta may be estimated from Eq. (5). The initial angular momenta l_i that couple to a given final angular momentum depend on the spin of the excited state. The mean values of the initial angular momenta appear to be restricted in the range $\langle l_f\rangle_{I_f} < \langle l_i\rangle_{I_f} < \langle l_f\rangle_{I_f} + I_f$. The reason for these restrictions seem to be the unitary limit of the total reaction cross section. For highly excited, high-spin states or for small fusion cross sections we found the even closer restriction $\langle l_i\rangle_{I_f} \approx \langle l_f\rangle_{I_f} + I_f$. It was argued that this relation is a condition for large cross section at large kinetic energy losses.

Besides these angular momentum considerations it was found that the energy dependence of the fusion cross section is in surprising agreement with the predictions of the simple model of Glas *et al.*[11] Although one cannot expect the interaction potentials obtained through this model to be more than only estimates of the real values, it still appears that the slope of the fusion cross section versus incident energy at large energies allows one to decide whether or not the interaction potential inside the nucleus is attractive or repulsive. To our knowledge the measurement of the fusion cross section is the only direct way to obtain this information.

The results of our calculations are also interesting in relation to the classical interpretation of heavy ion reactions. Frequently it is assumed that the quasielastic and deeply inelastic components of such reactions consist of excited states with opposite polarizations. This concept is intimately related to the classical deflection functions of heavy ion reactions.[20] It was pointed out that also our calculations suggest the existence of a possible polarization mechanism although of a different origin, namely due to the unitary limit of the total reaction cross section. A more detailed investigation, however, does not confirm the expectations of the extreme classical picture: The density matrices are nondiagonal and the expectation values of polarization are small. Furthermore, these values strongly vary with scattering angle. On the other hand, the alignment of nuclear states is found to be strong for low and high excitation energies. It is an unsolved problem whether this result is due to the particular properties of the $^{12}C + ^{24}Mg$ system and the potential used or whether this is a more gen-

eral property of heavy ion reactions. But it seems obvious that the interpretation of results in terms of classical pictures requires special caution.

One of us (D. P.) thanks the Weizmann Institute of Science for the kind hospitality he experienced during his stay there.

---

*Permanent address: Physikalisches Institut der Universität Heidelberg, D-6900 Heidelberg, Germany.

[1]R. S. Simon, M. V. Banaschik, R. M. Diamond, J. O. Newton, and F. S. Stephens, Nucl. Phys. A290, 253 (1977).
[2]W. U. Schröder, J. R. Birkelund, J. R. Huizenga, K. L. Wolf, and V. E. Viola, Phys. Rev. 16, 623 (1977).
[3]G. B. Hagemann, R. Broda, B. Hershkind, M. Ishahara, S. Ogaza, and H. Ryde, Nucl. Phys. A245, 166 (1975).
[4]D. G. Sarantites, J. H. Barker, M. L. Halbert, D. C. Hensley, R. A. Dayras, E. Eichler, N. R. Johnson, and S. A. Gronemeyer, Phys. Rev. C 14, 2138 (1976).
[5]T. Tamura, Rev. Mod. Phys. 37, 679 (1965).
[6]N. K. Glendenning, in Proceedings of the International School of Physics "Enrico Fermi", Course XL, Varenna Lectures, 1967, edited by M. Jean and R. A. Ricci (Academic, New York, 1969), p. 332.
[7]U. Smilansky, Nucl. Phys. A112, 185 (1968).
[8]J. Raynal, ICTP report, 1971 (unpublished).
[9]J. Wilczynski, Phys. Lett. 47B, 484 (1973).
[10]J. Galin, D. Guerreau, M. Lefort, and X. Tarrago, Phys. Rev. C 9, 1018 (1974).
[11]D. Glas and U. Mosel, Nucl. Phys. A237, 429 (1975).
[12]M. Tamir and M. Shapiro, Chem. Phys. Lett. 31, 166 (1975).
[13]A. E. DePristo and M. H. Alexander, J. Chem. Phys. 63, 3552 (1975).
[14]R. Vandenbosch, M. P. Webb, T. D. Thomas, and M. S. Zisman, Nucl. Phys. A269, 210 (1976); W. U. Schröder, J. R. Birkelund, J. R. Huizenga, K. L. Wolf, J. P. Unik, and V. E. Viola, Phys. Rev. Lett. 36, 514 (1976).
[15]R. G. Stokstad, Z. E. Switkowski, R. A. Dayras, and R. M. Wieland, Phys. Rev. Lett. 37, 888 (1976).
[16]P. Sperr, S. Vigdor, Y. Eisen, W. Henning, D. G. Kovar, T. R. Ophel, and B. Zeidman, Phys. Rev. Lett. 36, 405 (1976).
[17]I. Tserruya, Y. Eisen, D. Pelte, A. Gavron, H. Oeschler, D. Berndt, and H. L. Harney, Phys. Rev. C 18, 1688 (1978).
[18]R. Novotny, G. Hammer, D. Pelte, H. Emling, and D. Schwalm, Nucl. Phys. A294, 255 (1978).
[19]A. Olmi, H. Sann, D. Pelte, Y. Eyal, A. Gobbi, W. Kohl, U. Lynen, G. Rudolf, H. Stelzer, and R. Bock, Phys. Rev. Lett. 41, 688 (1978); P. Glässel, R. S. Simon, R. M. Diamond, R. C. Jared, I. Y. Lee, L. G. Moretto, J. O. Newton, R. Schmitt, and F. S. Stephens, *ibid.* 38, 331 (1977).
[20]F. Rybicki, T. Tamura, and G. R. Satchler, Nucl. Phys. A146, 659 (1970).